



A microfluidic-based electrochemical biochip for label-free diffusion-restricted DNA hybridization analysis

Hadar Ben-Yoav^{a,*}, Peter H. Dykstra^{a,1}, William E. Bentley^b, Reza Ghodssi^{a,b,**}

^a MEMS Sensors and Actuators Laboratory (MSAL), Department of Electrical and Computer Engineering, Institute for Systems Research, University of Maryland, College Park, MD 20742, United States

^b Fischell Department of Bioengineering, University of Maryland, College Park, MD 20742, United States

ARTICLE INFO

Article history:

Received 23 January 2012

Received in revised form

20 April 2012

Accepted 8 May 2012

Available online 16 May 2012

Keywords:

Electrochemical impedance spectroscopy

DNA hybridization biosensor

Biochip

Restricted diffusion

Microfluidics

Label-free detection

ABSTRACT

DNA hybridization detection in microfluidic devices can reduce sample volumes, processing times, and can be integrated with other measurements. However, as device footprints decrease and their complexity increase, the signal-to-noise ratio in these systems also decreases and the sensitivity is thereby compromised. Device miniaturization produces distinct properties and phenomena with greater influence at the micro-scale than at the macro-scale. Here, a diffusion-restriction model was applied to a miniaturized biochip nanovolume reactor to accurately characterize DNA hybridization events that contribute to shifts in both charge transfer resistance and diffusional resistance. These effects are shown to play a significant role in electrochemical impedance spectroscopy (EIS) analyses at these length scales. Our highly functional microfluidic biosensor enables the detection of ssDNA targets selectively, with a calculated detection limit of 3.8 nM, and cross-reactivity of 13% following 20 min incubation with the target. This new biosensing approach can be further modeled and tested elucidating diffusion behavior in miniaturized devices and improving the performance of biosensors.

© 2012 Elsevier B.V. All rights reserved.

1. Introduction

Clinical diagnostic tools have been used for decades in the field of DNA research. The detection of DNA hybridization events has great importance to numerous fields including cancer, influenza and genetics (Chee et al., 1996; Ito et al., 2007; Kallioniemi et al., 1994; Kao et al., 2011; Kukul et al., 2008; Ma et al., 2008). These traditional tools typically rely upon fluorescent or radioactive labels to produce a signal upon hybridization. Fluorescent labeling is common when using blotting techniques or a DNA microarray but requires additional sample preparation steps which increases the cost and time of the assay (Hardisson et al., 2004; Kim et al., 2006). Radioactive labeling requires highly trained personnel and carries additional safety risks (Grouse and Schrier, 1977).

Due to the added cost and difficulty associated with labeling, interest has grown in label-free sensing methods. These methods include the use of mechanical devices (Koev et al., 2007) such as

quartz crystal microbalances (QCMs) (Caruso et al., 1997; Lazerges et al., 2006), optical techniques like surface plasmon resonance (SPR) (Lao et al., 2009; Pollet et al., 2009) or electrical measurements taking advantage of the anionic charge present on DNA (Batchelor-McAuley et al., 2009; Guidotti et al., 2007; Lucarelli et al., 2004). Although very sensitive, QCM measurements are typically performed with a single sensor in an enclosed environment, making an array of such tests difficult. Likewise, SPR measurements are highly sensitive to binding events on a surface, but require expensive and bulky free space optics with precise temperature calibration to achieve stable output. Electrical sensors have been demonstrated for impedance, conductance or capacitance measurements of DNA hybridization and can be easily fabricated and integrated with common test equipment (Drummond et al., 2003; Gautier et al., 2007; Goral et al., 2006). Furthermore, the ability to pattern these sensors using traditional photolithography techniques makes them ideal for use in miniaturized systems. DNA hybridization events are electronically quantified using transducers such as electrodes or semiconductors. Electrochemical impedance spectroscopy (EIS) is one of the most common and effective methods to monitor time-dependent adsorption and assembly of nucleic acids on the transducer surface, and to characterize DNA hybridization events (Ju and Zhao, 2005; Katz and Willner, 2003; Revenga-Parra et al., 2011; Wang, 2002). This analysis requires initial surface functionalization of nucleic acids as the sensing interface, followed by

* Corresponding author. Tel.: +1 301 405 2168; fax: +1 301 314 9920.

** Corresponding author at: MEMS Sensors and Actuators Laboratory (MSAL), Department of Electrical and Computer Engineering, Institute for Systems Research, University of Maryland, College Park, MD 20742, United States. Tel.: +1 301 405 8158; fax: +1 301 314 9920.

E-mail addresses: benyoav@umd.edu (H. Ben-Yoav), ghodssi@umd.edu (R. Ghodssi).

¹ Hadar Ben-Yoav and Peter H. Dykstra contributed equally to this paper.

electronically transduced hybridization with the analyte DNA (Ensaifi et al., 2011; Gautier et al., 2007; Ito et al., 2007; Li et al., 2011; Wang et al., 2011). During the hybridization, a negatively charged interface is accumulated on the surface of the transducer that repels negatively charged electro-active species. This repulsion is transduced to higher impedance of the electron transfer reaction at the interface, hence increases the charge transfer resistance.

While the majority of published literature on electrochemical-based DNA hybridization analysis discusses experiments performed in beakers of solution with a high signal-to-noise ratio and a low background signal, there is a growing trend of using microfluidic devices for electrochemical detection of DNA hybridization (Dukkipati and Pang, 2006; Fang et al., 2009; Pavlovic et al., 2008; Xu et al., 2009). Microfluidic-based lab-on-a-chip devices have the potential for functional integration with other technologies and miniaturization, leading to portability, high-throughput usage, and low-cost mass production. These devices use low sample volumes, provide fast reaction rates due to the smaller diffusion distances, are inexpensive to produce and can include integrated sensors to provide label-free analysis (Hong et al., 2009; Yang and Woolley, 2010). However, the miniaturized device footprints increase their complexity, hence the signal-to-noise ratio decreases and the sensitivity is thereby compromised. Furthermore, distinct properties and phenomena with greater influence at the micro-scale than at the macro-scale are resulted by this miniaturization (Beebe et al., 2002). The emergence of these factors at the micro-scale contributes to the often counter-productive nature of shrinking existing large devices and expecting maintained performance. Dominant properties unique to microfluidic environments include laminar flow (Brody et al., 1996; Koo and Kleinstreuer, 2003; Purcell, 1977; White, 1991), diffusion (Du et al., 2009; Jiang et al., 2005; Liu et al., 2000; Weigl and Yager, 1999), fluidic resistance (Kovacs, 1998; White, 1991), surface area to volume ratio (Browne et al., 2011; Chen et al., 2010; Locascio et al., 1999; Manz et al., 1994), and surface tension (Junghoon and Chang-Jin, 2000; Pollack et al., 2000; Prins et al., 2001; Zhao et al., 2001). By taking advantage of these effects with miniaturized lab-on-a-chip sensing devices, one can develop new sensing approaches that will improve the overall performance of biosensors.

Here we present a microfluidic-based electrochemical biochip, which contains an array of individually addressable 25 nL reaction chambers, fabricated with micro-electromechanical systems (MEMS) technology. Three unique single stranded DNA (ssDNA, 30-mers) probes were functionalized onto patterned electrodes of the chip to detect complementary DNA hybridization events using EIS analysis. The DNA hybridization events were tested with both macro- and micro-biochips and demonstrated the specificity and the functionality of the biosensor. The miniaturization of the biochip's reaction chamber volume from the macro- to the nano-scale regime intensifies the effect of diffusion on the performance of the sensing mechanism. Restricted diffusion-based electrical models (Bisquert and Compte, 2001) have been used to characterize electrochemical systems, such as electron recombination in thin layers (Bisquert, 2001), nanoporous materials in nonaqueous solutions (Jānes and Lust, 2006), Lithium insertion–deinsertion mechanism (Quintin et al., 2006), electronic and ionic processes in dye-synthesized solar cells (Wang et al., 2005), and bacterial biofilm development monitoring (Ben-Yoav et al., 2011). Here the restricted diffusion-based electrical model was used for the first time to analyze DNA hybridization events, in oppose to the commonly used semi-infinite diffusion model (Bisquert et al., 1999; Randles, 1947; Sluythters-Rehbach and Sluythters, 1984; Vetter, 1967; Warburg, 1901), harnessing the dominant influence of the reaction chamber nanovolume on

molecular diffusion. Results demonstrated both diffusion-based and charge transfer-based components of the observed impedance influenced by the DNA hybridization events.

2. Materials and methods

2.1. DNA, solutions and instruments

All ssDNA sequences were purchased from Integrated DNA Technologies (Coralville, IA). Three probe sequences (ssDNA1, 5'-HS-(CH₂)₆-AAAGCTCCGATAGCGCTCCGTGGACGTCCC-3'; ssDNA2, 5'-HS-(CH₂)₆-ACGCGTCAGGTCATTGACGAATCGATGAGT-3'; ssDNA3, 5'-HS-(CH₂)₆-ACCTAGATCCAGTAGTTAGACCCATGATGA-3') and three complementary target sequences (t-DNA1, 5'-GGGACGTCCACGGA GCGCTATCGGAGCTTT-3'; t-DNA2, 5'-ACTCATCGATTTCGTAATGACCT-GACCCGT-3'; t-DNA3, 5'-TCATCATGGGTCTAACTACTGGATCTAGGT-3') were each re-suspended in a buffer solution containing 10 mM Tris, 50 mM NaCl and 1 mM EDTA and frozen at -20 °C in 20 μL aliquots until further use. 6-mercapto-1-hexanol (MCH), and Tris (2-carboxyethyl) phosphine (TCEP) were each purchased from Sigma-Aldrich (St. Louis, MO). Buffers for all experiments were either 10 mM phosphate buffer solution (PBS) with 100 mM NaCl or 4 × saline sodium citrate (SSC). All electrochemical tests were performed with a CHI660D single channel potentiostat from CH Instruments (Austin, TX). An Ag/AgCl reference electrode with 1 M KCl electrolyte and a platinum wire as a counter electrode were also purchased from CH Instruments. The electrolyte used in all impedance experiments was 10 mM PBS with 100 mM added NaCl and included 2.5 mM ferricyanide and 2.5 mM ferrocyanide as a reversible redox couple.

2.2. Biochip design and fabrication

The electrode layout is designed to provide individually addressable working electrodes within an array. The design used in this work contains nine sensors patterned in a 3 × 3 grid previously shown by Dykstra et al. (2011) as a platform for protein adsorption analysis. Each row of three sensors (each working electrode is a disk of 100 μm radius, and they spaced 5 mm apart in the row) also contains a counter and reference electrode to complete the three-electrode system. Gold is used for the counter and working electrodes while platinum is chosen for the reference electrode; the thiol groups from the probe ssDNA self assemble and form strong covalent bonds with the gold surface, and platinum has been demonstrated previously to provide a stable reference potential (Pavlovic et al., 2008). The electrodes are arranged in a grid format to expose either rows or columns of electrodes, dependent on the microfluidic channel orientation. In this way, multiple sensor surfaces can be functionalized with specific probes without cross-contamination, and multiple samples can be incubated with the probe sequences in parallel. The sensor grid design is easily scalable using micro-fabrication techniques to include many more sensors than the nine demonstrated here. The 3 × 3 grid is chosen to demonstrate the proof-of-concept capability for DNA hybridization.

The fabrication procedure for the biochip has been previously described (Dykstra et al., 2011). Briefly, electrodes are patterned onto a silicon dioxide substrate via DC sputtering and E-beam evaporation and patterned using both wet etching and lift-off techniques. The microfluidic channels (100 μm in height and 500 μm in width) are cast in a 10:1 ratio of polydimethylsiloxane (PDMS) over a mold of patterned SU8-50. The curing is performed in an oven at 80 °C for 20 min. After carefully peeling the PDMS away from the mold, fluid inlets of 1 mm radius are punched through the PDMS. The PDMS is aligned by eye over the patterned electrodes so that each electrode in a row or column lies in its

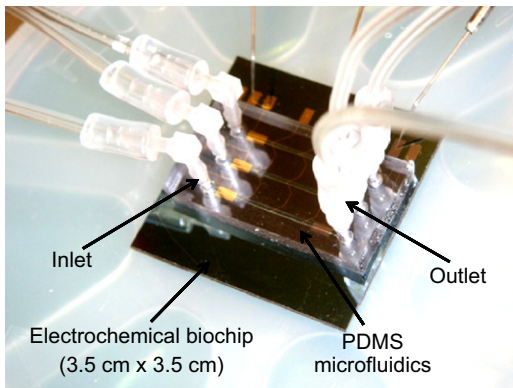


Fig. 1. Photograph of packaged device under test (chip dimensions: 3.5 cm × 3.5 cm. Micro-channel height was 100 μm and 500 μm in width).

own separate reaction nano-chamber. The resulting reaction chambers hold 25 nL volume each. The reversible bond of the PDMS to the silicon dioxide surface provides a leak-proof seal during the experiments. Micropositioning probes make electrical contact to pads on the outer edge of the chip. The completed device is shown in Fig. 1.

2.3. DNA hybridization analysis using electrochemical impedance spectroscopy

Two different types of tests were performed in this work. The first was conducted in a beaker of electro-active solution (PBS with added ferricyanide/ferrocyanide couple) using macro-scale gold electrodes (1 mm radius working disk electrode), a platinum wire as a counter electrode, and an Ag/AgCl reference electrode. These tests confirmed the selectivity amongst the various DNA sequences using electrochemical measurements. The second test used the microfluidic-based biochip to perform the same DNA hybridization experiments in an arrayed format. For the macro-scale tests, electrodes were incubated in a solution containing 10 mM PBS, 100 mM NaCl, 10 μM TCEP and 1 μM probe ssDNA for 1 h followed by rinsing with PBS. Afterwards, the electrodes were incubated for 1 h in PBS solution containing 1 mM of MCH. MCH is used to passivate any exposed regions on the surface to reduce non-specific binding effects during DNA sensing (Kukol et al., 2008; McEwen et al., 2009; Sumner et al., 2005; Xiao et al., 2006). Impedance measurements were performed in the frequency range from 0.1 MHz to 1 Hz (12 frequency data points per frequency decade, 5 mV amplitude) in a 10 mL beaker after each incubation with each of the three target ssDNA sequences, where the working electrode was polarized at 185 mV (open circuit potential) vs. Ag/AgCl. Incubation with the target sequences was performed in a 4 × SSC buffer containing 1 μM of the target DNA for 20 min. For the microfluidic-based biochip tests, the PDMS mold with 3 parallel micro-channels was first aligned to expose 3 separate vertical micro-channels of 3 working electrodes each. Each micro-channel was filled with a different solution containing different type of probe ssDNA and allowed to incubate for 1 h, followed by flushing with PBS and subsequent incubation with 1 mM MCH. In this way, each vertical micro-channel of 3 electrodes was functionalized with a different ssDNA probe sequence. After each channel was washed with PBS, the PDMS was lifted off, rotated 90° to a horizontal orientation, and placed down to expose separate rows of reaction nano-chambers with each row containing a unique counter and reference electrode. Impedance measurements were taken from each electrode before and after incubation with a target ssDNA sequence for 20 min. Impedance measurements were performed in the frequency range from

1 MHz to 0.1 Hz (10 frequency data points per frequency decade, 25 mV amplitude) where the working electrode was polarized at 5 mV (open circuit potential) vs. Ag/AgCl. The target ssDNA is able to interact with each uniquely functionalized sensor surface in the channel. All impedance spectroscopy experiments were performed in triplicates.

3. Results and discussion

3.1. DNA hybridization analysis using macro-scale setup

EIS biosensors are very sensitive to small electrochemical changes at the electrode–electrolyte interface. EIS-based DNA biosensors detect hybridization events that occur at the interface of the electrode. However, the miniaturization of the device's reaction chamber volume from the macro- to the nano-scale regime intensifies the effect of diffusion on the performance of the sensing mechanism. These effects are dominant when the diffusion layer thickness is on the same order as the reaction chamber features, as is the case in the microfluidic sensing biochip presented here. For example, the nano-chamber 'ceiling' acts as a reflecting border for the electro-active species diffusing in the system resulting in variations with its intrinsic diffusion mechanism (Fig. 2). The performance of the EIS-based DNA biosensor was characterized with both macro- and micro-scale biochips. The response time of DNA hybridization events were characterized (shown in Supplementary data 1). The Warburg diffusion-controlled electrical model (Bisquert et al., 1999; Randles, 1947; Sluythters-Rehbach and Sluythters, 1984; Vetter, 1967; Warburg, 1901) was used to analyze the specificity of the biosensor in the macro-scale system. Afterwards, the microfluidic-based biochip was used to study the specificity and the functionality of DNA hybridization events with a modified restricted diffusion-based (Bisquert and Compte, 2001) electrical circuit model to include the dominant influence of the reflecting chamber "ceiling" on the electro-active diffusion in the miniaturized system.

The specificity of the biosensor was initially tested with macro-scale electrodes where the binding selectivity of three different ssDNA targets for three different complementary ssDNA probes was examined. Impedance measurements of the reactions between different ssDNA targets with three different ssDNA probes are presented as three Nyquist plots (corresponding to the three different ssDNA probes) in Fig. 3A. The results

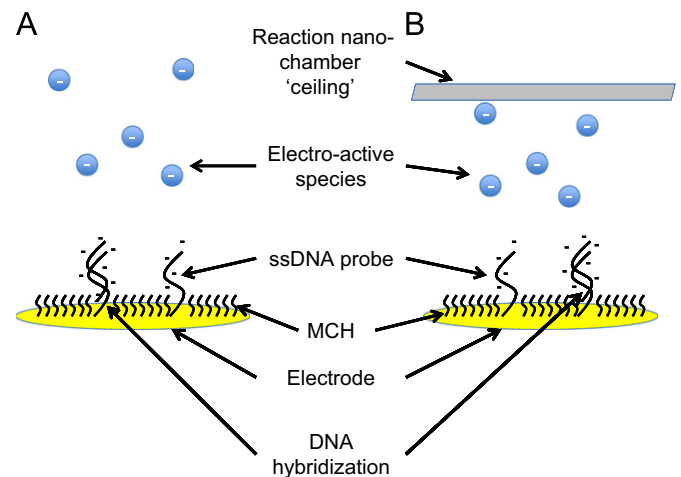


Fig. 2. Schematics of the diffusion-based biosensing approach for (A) macro-scale biochips and (B) microfluidic-based biochips, highlighting the additional reflective boundary present in the microfluidic biochips.

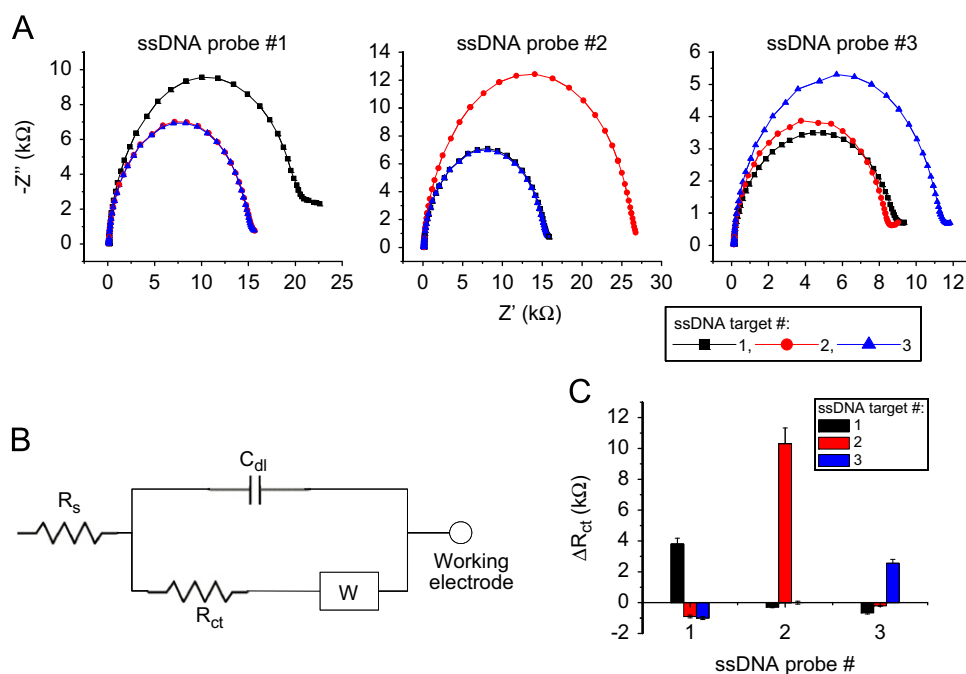


Fig. 3. Impedance spectroscopy measurements of DNA hybridization on macro-scale electrodes. (A) Nyquist plots of impedance measurements of three different ssDNA probes following incubation with three different complementary and non-complementary ssDNA targets. (B) Diagram of Randles cell electrical circuit that was used for impedance spectroscopy analysis. R_s is the solution resistance, R_{ct} is the charge transfer resistance, C_{dl} is the electrode–electrolyte double layer interface, and W is Warburg diffusion. (C) The difference of the calculated charge transfer resistance before and after incubation period with three different ssDNA targets for three different ssDNA probes.

demonstrate the measured differences between complementary and non-complementary ssDNA targets. The resulting impedance spectroscopy measurements were fitted to the equivalent electrical circuit of the Randles cell (Randles, 1947) (for circuit schematics refer to Fig. 3B) using CHI660D software v11.08, CH Instruments Inc., USA. The Randles cell model was used to signify the polarizable electrode interface, based on the assumptions that a diffusion restriction does not exist, a simple single-step electrochemical reaction takes place on the working electrode surface, and the contribution of the counter electrode to the impedance measurement is negligible due to its significantly higher surface. The difference between the calculated R_{ct} before and after incubation with either non-complementary or complementary ssDNA targets for three different ssDNA probes ($\Delta R_{ct} = R_{ct,after\ incubation} - R_{ct,before\ incubation}$) is shown in Fig. 3C. The results demonstrate higher ΔR_{ct} values when the complementary ssDNA target was introduced, therefore presenting high probe-target specificity and little non-specific binding on the biosensor.

3.2. Microfluidic-based biochip for DNA hybridization analysis

Miniaturization of electrochemical lab-on-a-chip devices increases the effect of the surrounding reaction chamber features on the electro-active species diffusion in the system. In macro-scale systems, the dominating diffusion element is the Warburg semi-infinite ordinary linear diffusion (Armstrong et al., 1973; Randles, 1947; Warburg, 1901). This element is obtained using the Nernstian boundary condition where a steady-state condition occurs at infinity, i.e. $\Delta c(\infty) = 0$. Miniaturization of the electrochemical lab-on-a-chip features, e.g. reaction chamber and electrode dimensions, affects the boundary conditions hence varying the intrinsic diffusion characteristics. Therefore, using a restricted diffusion model instead of a semi-infinite diffusion model provides a more accurate representation of the electrochemical system in miniaturized lab-on-a-chip devices. The restricted diffusion model is a modified bioelectrical model using a restricted linear ordinary diffusion impedance element with a reflective boundary (Bisquert

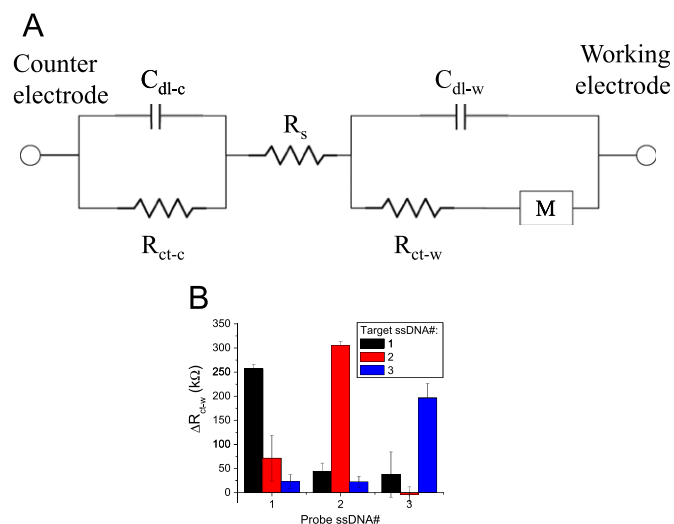


Fig. 4. (A) Proposed diffusion-restricted bioelectrical equivalent circuit. (B) The difference of the calculated charge transfer resistance at the working electrode following incubation with different ssDNA targets with three different ssDNA probes.

and Compte, 2001) to characterize for the first time a new biosensing approach for DNA hybridization analysis using a microfluidic-based biochip (for circuit schematics refer to Fig. 4A). The anomalous diffusion theory used here to model the effect where some particles in the electrolyte are reflected by the nano-chamber walls during an ordinary linear diffusion behavior in opposed to the Warburg diffusion in a macro-scale system.

The bioelectrical model includes both energy storage and dissipation elements. R_s is the solution resistance, R_{ct} is the charge transfer resistance (subscript-c at the counter electrode, subscript-w at the working electrode), C_{dl} is the electrode–electrolyte double layer interface (subscript-c at the counter electrode, subscript-w at the working electrode), and M is the restricted linear diffusion impedance element with a reflective boundary (Bisquert and

Compte, 2001) due to physical and chemical interactions between particles and ions in the electrolyte and the components of the electrochemical system. The counter electrode is included in the model, as opposed to the macro-scale system, as its surface area is at the same order of magnitude as the working electrode. The corresponding impedance elements are described in Supplementary data 2.

The performance of the microfluidic DNA biochip was studied. The selectivity was tested by implementing the same overall strategy employed at the macro-scale system. Each of the three ssDNA sequences was introduced into each channel of the microfluidic-based biochip comprised of different sensory reaction nano-chambers with immobilized ssDNA probes. The change of the electrical signal due to DNA hybridization was monitored with impedance spectroscopy using the ferricyanide/ferrocyanide couple dissolved in PBS. Fig. 4B shows the difference between the calculated R_{ct-w} before and after incubation with either a non-complementary or a complementary ssDNA target for three different ssDNA probes on the same biochip ($\Delta R_{ct-w} = R_{ct-w,after\ incubation} - R_{ct-w,before\ incubation}$). The results demonstrated higher ΔR_{ct-w} values when the complementary ssDNA target was introduced. Furthermore, an average of 13% cross-reactivity ($Cross-reactivity = \Delta R_{ct-w,non-complementary\ ssDNA} / \Delta R_{ct-w,complementary\ ssDNA}$) value was resulted in the presence of the non-complementary ssDNA in all different probes. The selectivity of the impedance measurements to the presence of the complementary target ssDNA is due to the increase of the repulsion force between the DNA and the electro-active species (ferrocyanide and ferricyanide) present in the electrolyte (Katz and Willner, 2003). The stronger repulsive forces make diffusion more difficult

for electro-active species, reflected by the increase in the calculated charge transfer resistance (R_{ct-w}) values.

The sensitivity of the biosensor was tested by incubating probe ssDNA with different concentrations of complementary ssDNA target. Impedance measurements for increasing complementary ssDNA target concentrations are presented as a Nyquist plot in Fig. 5A. The results demonstrate a trend of increasing impedance values measured at low frequencies (~ 15 Hz) for increasing ssDNA target concentrations.

The resulting impedance spectroscopy measurements were fitted to the proposed equivalent bioelectrical circuit (Fig. 4A) using EC-Lab v10.18, Bio-Logic-Science Instruments, France. The calculated charge transfer resistance and the restricted diffusional resistance at the working electrode as a function of the complementary ssDNA target concentration are shown in Fig. 5B and C respectively. The results show a semilogarithmic relation, with a slope of $25497.0 \pm 0.3 \Omega$ and an intercept of $139942.5 \pm 0.4 \Omega$, between the calculated charge transfer resistance at the working electrode and the ssDNA target concentration (Fig. 5B). The theoretical limit of detection was determined to be 4.7 nM by the calculation of the corresponding ssDNA target concentration for the background signal.

The calculated restricted diffusional resistance shows semilogarithmic dependence with the ssDNA target concentration (Fig. 5C), with a slope of $11355.0 \pm 2.6 \Omega$ and an intercept of $234324 \pm 3 \Omega$. The theoretical limit of detection was determined to be 3.8 nM, which resulted at least the same sensitivity as the charge transfer resistance analysis, by the calculation of the corresponding ssDNA target concentration for the background signal. These results suggest that the electro-active diffusion

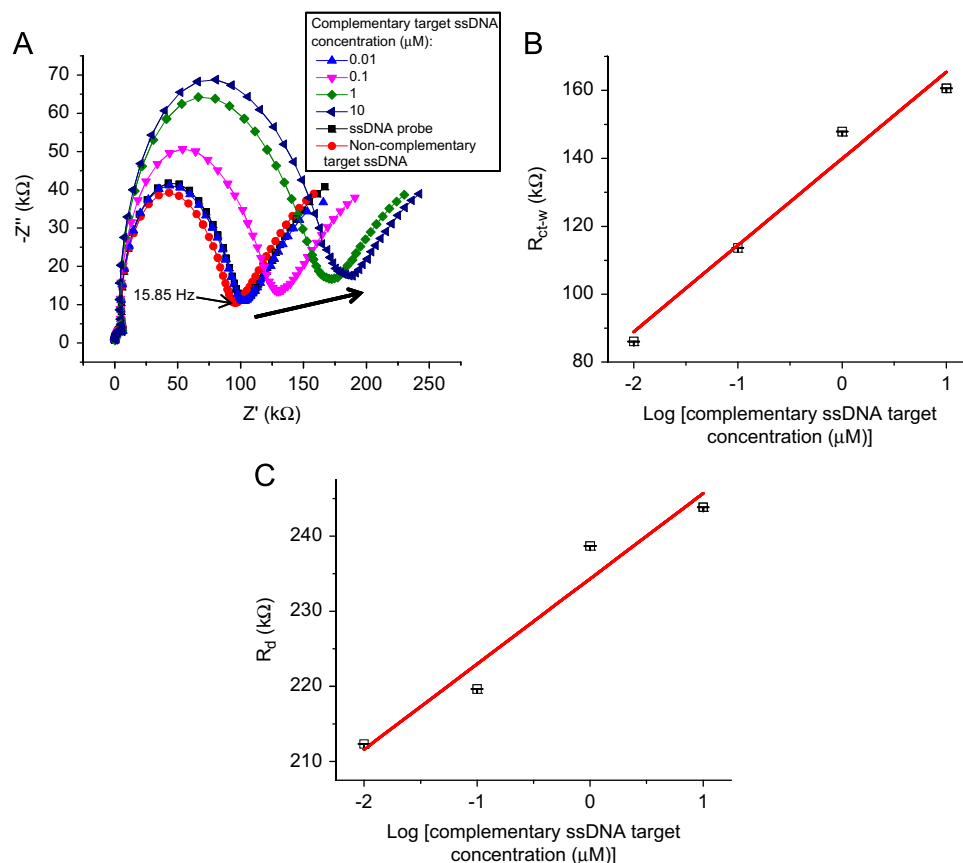


Fig. 5. The influence of the concentration of the complementary ssDNA target on the biosensing mechanism following incubation with 0.01, 0.1, 1, and 1 μ M target ssDNA. (A) Nyquist plot of impedance spectroscopy measurements (Arrow indicates increasing ssDNA target concentrations). The influence of the complementary ssDNA target concentration on the calculated (B) charge transfer resistance at the working electrode— R_{ct-w} (coefficient of variation=31%) and (C) restricted diffusional resistance— R_d (coefficient of variation=7%) components.

characteristics were affected by the DNA hybridization biosensing mechanism and could be monitored with EIS. A higher number of DNA hybridization events result in stronger electrostatic repulsion forces that may decrease the diffusion coefficient of the affected electro-active species. As the diffusion coefficient is inversely proportional to the diffusional resistance (Bisquert and Compte, 2001), higher resistance values were depicted. By further monitoring and improving the influence of diffusion-restricted effects, a new biosensing analysis approach can be used to improve the sensitivity and the functionality of the biosensor.

4. Conclusions

In this study, a microfluidic-based biochip for diffusion-restricted DNA hybridization analysis using EIS was presented. The biosensor performance and sensitivity were evaluated with macro-scale electrodes and an arrayed-based microfluidic biochip, demonstrated a robust and sensitive DNA biosensor. By the integration of the functional and the specific characteristics of the biosensor along with the advantages of miniaturized devices (i.e. cost-effective, easy to operate, low sample volume, multi-marker analysis, and fast reaction time) over classical molecular biology techniques, a new class of portable biosensors for rapid analysis of DNA is resulted. The new miniaturized biosensor is a cost-effective, high throughput, and easy to operate system, that requires low sample volume, has fast reaction times, for multi-marker analysis. However, the low signal-to-noise ratio, the high background signal, and the low stability of the system may compromise the sensitivity and the performance of the biosensor. By further improvement of DNA hybridization efficiency, e.g. ionic strength of the electrolyte and ssDNA probe assembly, the performance and sensitivity can be improved. Moreover, due to the high sensitivity of the biosensor for charge variations, detection of base-pair mismatches can be examined as one of the potential applications.

Miniaturization of electrochemical lab-on-a-chip devices results in physical and chemical fundamental variations that can be analyzed with EIS. One of the dominant effects of miniaturization is on the intrinsic diffusion characteristics. A new biosensing approach to monitor DNA hybridization events by diffusion analysis was demonstrated. A restricted linear diffusion model was utilized accounting for the effect of nanovolume reaction chamber features on the diffusion boundary layer. The unique analysis of the influence of DNA hybridization events on the diffusion characteristics as opposed to the conventional approaches can improve the overall biosensor performance due to the dominant diffusion characteristics in the micro-scale. This analysis resulted detection limit is at least the same as the conventional charge transfer analysis. By integrating these effects into a more rigorous bioelectrical model, diffusion characteristics can be monitored during DNA hybridization events. Supplementary modeling and testing of the presented new biosensing approach can elucidate diffusion behavior in miniaturized devices and improving the performance of the biosensor. Further analysis of the diffusion in these devices can improve the diversity, the sensitivity, and the time of operation of biosensors.

Acknowledgments

The authors acknowledge the Robert W. Deutsch Foundation and National Science Foundation Emerging Frontiers in Research and Innovation (EFRI) for financial support. The authors also thank the Maryland Nanocenter and its Fablab for cleanroom facility support.

Appendix A. Supporting information

Supplementary data associated with this article can be found in the online version at doi:10.1016/j.bios.2012.05.009.

References

- Armstrong, R.D., Firman, R.E., Thirsk, H.R., 1973. *Faraday Discussions of the Chemical Society* 56, 244–263.
- Batchelor-McAuley, C., Wildgoose, G.G., Compton, R.G., 2009. *Biosensors and Bioelectronics* 24 (11), 3183–3190.
- Beebe, D.J., Mensing, G.A., Walker, G.M., 2002. *Annual Review of Biomedical Engineering* 4 (1), 261–286.
- Ben-Yoav, H., Freeman, A., Sternheim, M., Shacham-Diamand, Y., 2011. *Electrochimica Acta* 56 (23), 7780–7786.
- Bisquert, J., 2001. *The Journal of Physical Chemistry B* 106 (2), 325–333.
- Bisquert, J., Compte, A., 2001. *Journal of Electroanalytical Chemistry* 499 (1), 112–120.
- Bisquert, J., Garcia-Belmonte, G., Fabregat-Santiago, F., Bueno, P.R., 1999. *Journal of Electroanalytical Chemistry* 475 (2), 152–163.
- Brody, J.P., Yager, P., Goldstein, R.E., Austin, R.H., 1996. *Biophysical Journal* 71 (6), 3430–3441.
- Browne, A.W., Ramasamy, L., Cripe, T.P., Ahn, C.H., 2011. *Lab on a Chip* 11 (14), 2440–2446.
- Caruso, F., Rodda, E., Furlong, D.N., Haring, V., 1997. *Sensors and Actuators B: Chemical* 41, 189–197.
- Chee, M., Yang, R., Hubbell, E., Berno, A., Huang, X.C., Stern, D., Winkler, J., Lockhart, D.J., Morris, M.S., Fodor, S.P.A., 1996. *Science* 25, 610–614.
- Chen, C.H., Lu, Y., Sin, M.L.Y., Mach, K.E., Zhang, D.D., Gau, V., Liao, J.C., Wong, P.K., 2010. *Analytical Chemistry* 82 (3), 1012–1019.
- Drummond, T.G., Hill, M.G., Barton, J.K., 2003. *Nature Biotechnology* 21 (10), 1192–1199.
- Du, Y., Shim, J., Vidula, M., Hancock, M.J., Lo, E., Chung, B.G., Borenstein, J.T., Khabiry, M., Crokek, D.M., Khademhosseini, A., 2009. *Lab on a Chip* 9 (6), 761–767.
- Dukkipati, V.R., Pang, S.W., 2006. *Integrated microfluidic system for DNA analysis. Nanotechnology, Cincinnati, OH Osteopathic Hospitals*. pp. 162–165.
- Dykstra, P.H., Roy, V., Byrd, C., Bentley, W.E., Ghodssi, R., 2011. *Analytical Chemistry* 83 (15), 5920–5927.
- Ensaifi, A.A., Taei, M., Rahmani, H.R., Khayamian, T., 2011. *Electrochimica Acta* 56 (24), 8176–8183.
- Fang, T.H., Ramalingam, N., Xian-Dui, D., Ngai, T.S., Xianting, Z., Kuan, A.T.L., Huat, E.Y.P., Hai-Qing, G., 2009. *Biosensors and Bioelectronics* 24, 2131–2136.
- Gautier, C., Esnault, C., Cougnon, C., Pilard, J.-F., Casse, N., Chenais, B., 2007. *Journal of Electroanalytical Chemistry* 610, 227–233.
- Goral, V.N., Zaytseva, N.V., Baeumner, A.J., 2006. *Lab on a Chip* 6, 414–421.
- Grouse, L.D., Schrier, B.K., 1977. *Analytical Biochemistry* 79, 95–103.
- Guidotti, C., Minunni, M., Moncelli, M.R., 2007. *Electrochemistry Communications* 9, 2380–2386.
- Hardisson, D., Alvarez-Marcos, C., Salas-Bustamante, A., Alonso-Guervós, M., Sastre, N., Sampedro, A., 2004. *Oral Oncology* 40, 409–417.
- Hong, J., Edel, J.B., deMello, A.J., 2009. *Drug Discovery Today* 14, 134–146.
- Ito, T., Hosokawa, K., Maeda, M., 2007. *Biosensors and Bioelectronics* 22, 1816–1819.
- Janes, A., Lust, E., 2006. *Journal of the Electrochemical Society* 153 (1), A113–A116.
- Jiang, X., Xu, Q., Dertinger, S.K.W., Stroock, A.D., Fu, T.-M., Whitesides, G.M., 2005. *Analytical Chemistry* 77 (8), 2338–2347.
- Ju, H., Zhao, H., 2005. *Frontiers in Bioscience: A Journal and Virtual Library* 10, 37–46.
- Junghoon, L., Chang-Jin, K., 2000. *Journal of Microelectromechanical Systems* 9 (2), 171–180.
- Kallioniemi, A., Kallioniemi, O.-P., Piper, J., Tanner, M., Stokke, T., Chen, L., Smith, H.S., Pinkel, D., Gray, J.W., Waldman, F.M., 1994. *Proceedings of the National Academy of Sciences* 91, 2156–2160.
- Kao, L.T.-H., Shankara, L., Kanga, T.G., Zhanga, G., Taya, G.K.I., Rafeia, S.R.M., Lee, C.W.H., 2011. *Biosensors and Bioelectronics* 26, 2006–2011.
- Katz, E., Willner, I., 2003. *Electroanalysis* 15 (11), 913–947.
- Kim, J.H.-S., Marafie, A., Jia, X.-Y., Zoval, J.V., Madou, M.J., 2006. *Sensors and Actuators B: Chemical* 113, 281–289.
- Koev, S.T., Powers, M.A., Yi, H., Wu, L.-Q., Bentley, W.E., Rubloff, G.F., Payne, G.F., Ghodssi, R., 2007. *Lab on a Chip* 7, 103–111.
- Koo, J., Kleinstreuer, C., 2003. *Journal of Micromechanics and Microengineering* 13 (5), 568–579.
- Kovacs, G.T.A., 1998. *Micromachined Transducers Sourcebook*. McGraw-Hill, Boston.
- Kukol, A., Li, P., Estrela, P., Ko-Ferrigno, P., Migliorato, P., 2008. *Analytical Biochemistry* 374, 143–153.
- Lao, A.I.K., Su, X., Aung, K.M.M., 2009. *Biosensors and Bioelectronics* 24, 1717–1722.
- Lazerges, M., Perrot, H., Zeghib, N., Antoine, E., Compere, C., 2006. *Sensors and Actuators B: Chemical* 120, 329–337.
- Li, F., Han, X., Liu, S., 2011. *Biosensors and Bioelectronics* 26 (5), 2619–2625.

- Liu, R.H., Stremler, M.A., Sharp, K.V., Olsen, M.G., Santiago, J.G., Adrian, R.J., Aref, H., Beebe, D.J., 2000. *Journal of Microelectromechanical Systems* 9 (2), 190–197.
- Locascio, L.E., Perso, C.E., Lee, C.S., 1999. *Journal of chromatography A* 857 (1–2), 275–284.
- Lucarelli, F., Marrazza, G., Turner, A.P.F., Mascini, M., 2004. *Biosensors and Bioelectronics* 19, 515–530.
- Ma, Y., Jiao, K., Yang, T., Sun, D., 2008. *Sensors and Actuators B: Chemical* 131, 565–571.
- Manz, A., Effenhauser, C.S., Burggraf, N., Harrison, D.J., Seiler, K., Fluri, K., 1994. *Journal of Micromechanics and Microengineering* 4 (4), 257–265.
- McEwen, G.D., Chen, F., Zhou, A., 2009. *Analytica Chimica Acta* 643, 26–37.
- Pavlovic, E., Lai, R.Y., Wu, T.T., Ferguson, B.S., Sun, R., Plaxico, K.W., Soh, H.T., 2008. *Langmuir* 24 (3), 1102–1107.
- Pollack, M.G., Fair, R.B., Shenderov, A.D., 2000. *Applied Physics Letters* 77 (11), 1725–1726.
- Pollet, J., Delpont, F., Janssen, K.P.F., Jans, K., Maes, G., Pfeiffer, H., Wevers, M., Lammertyn, J., 2009. *Biosensors and Bioelectronics* 25, 864–869.
- Prins, M.W.J., Welters, W.J.J., Weekamp, J.W., 2001. *Science* 291 (5502), 277–280.
- Purcell, E.M., 1977. *American Journal of Physics* 45 (1), 3–11.
- Quintin, M., Devos, O., Delville, M.H., Campet, G., 2006. *Electrochimica Acta* 51 (28), 6426–6434.
- Randles, J.E.B., 1947. *Discussions of the Faraday Society* 1, 11–19.
- Revenga-Parra, M., Garcia, T., Pariente, F., Lorenzo, E., Alonso, C., 2011. *Electroanalysis* 23 (1), 100–107.
- Sluythens-Rehbach, M., Sluythens, J.H., 1984. In: Yeager, E., Bockris, J.O.M., Conway, B.A., Sarangapani, S. (Eds.), *Comprehensive Treatise of Electrochemistry*, vol. 9. Plenum Press, New York, pp. 177–292.
- Sumner, J.J., Plaxico, K.W., Meinhart, C.D., Soh, H., 2005. In: Cullum, B.M., Carter, J.C. (Eds.), *Development of an electrochemical biosensor without a sandwich assay*. SPIE.
- Vetter, K.J., 1967. *Electrochemical Kinetics*. Academic Press, New York.
- Wang, J., 2002. *Analytica Chimica Acta* 469 (1), 63–71.
- Wang, Q., Moser, J.-E., Grätzel, M., 2005. *The Journal of Physical Chemistry B* 109 (31), 14945–14953.
- Wang, Q., Zhang, B., Lin, X., Weng, W., 2011. *Sensors and Actuators B: Chemical* 156 (2), 599–605.
- Warburg, E., 1901. *Annalen der Physik* 311 (9), 125–135.
- Weigl, B.H., Yager, P., 1999. *Science* 283 (5400), 346–347.
- White, F.M., 1991. *Viscous Fluid Flow*, second ed. McGraw-Hill, Boston.
- Xiao, Y., Lubin, A.A., Baker, B.R., Plaxico, K.W., Heeger, A.J., 2006. *Proceedings of the National Academy of Sciences* 103 (45), 16677–16680.
- Xu, X., Zhang, S., Chen, H., Kong, J., 2009. *Talanta* 80, 8–18.
- Yang, W., Woolley, A.T., 2010. *Journal of Laboratory Automation* 15, 198–209.
- Zhao, B., Moore, J.S., Beebe, D.J., 2001. *Science* 291 (5506), 1023–1026.